THERMODYNAMIC ANALYSIS OF THE OFF-DESIGN PERFORMANCE OF A MICRO SOLAR ORGANIC RANKINE CYCLE TRIGENERATION SYSTEM

Ramin Moradi[1], Pietro Elia Campana[2], Roberto Tascioni[1], Luca Cioccolanti[1,*]

[1] Università eCampus, Centro di Ricerca per l'Energia, l'Ambiente e il Territorio, Novedrate (CO), Italy

[2] Malardalen University, Department of Sustainable Energy Systems, Vasterås, Sweden

*Corresponding Author: luca.cioccolanti@uniecampus.it

ABSTRACT

Organic Rankine Cycle (ORC) systems are considered as one of the most suitable technologies to produce electricity from low-temperature sources. ORC units can efficiently convert low-temperature solar energy into electric and thermal power. Independently from the solar technology used, the hourly and the seasonal fluctuations of solar energy entail challenging dynamic effects and bring these systems to operate in off-design conditions. Such effects are even more influential at micro-to-small scales granting paramount importance to the comprehensive understanding of their behavior.
In this study, the annual performances of a 4 kWe/50 kWth solar ORC trigenerative system for residential applications are numerically investigated. Four different modeling approaches commonly used in annual system-level simulations of ORC systems are compared. These models differ in the system-level modeling approach and the components modeling method. The analysis has shown that the simplest ORC model results in the lowest discrepancy compared to the model with the least assumption, in which the components are modeled empirically, and the high and low pressures of the system are found iteratively. The difference between the produced electric energy using the four models is significantly higher in hot months, in which the average temperature of the water tank is high due to the requirements of the vapor generator of the absorption chiller. In this case, the expander pressure ratio drops drastically depending on the system model algorithm, which affects the produced electric power depending on the adopted expander model. On the contrary, the discrepancy between the models for the produced thermal energy is negligible.

1 INTRODUCTION

Solar energy is one of the most promising renewable sources for a carbon-free society. In the last decades, many efforts have been put to make traditional solar technologies such as solar thermal panels and photovoltaic systems more efficient and cost competitive. However, when cooling, heating, and electrical energies are demanded such as in residential applications, solar combined cooling heat and power (CCHP) systems are preferred. Besides hybrid photovoltaic thermal systems (PVT), Organic Rankine Cycle (ORC) systems are attracting a lot of interest recently to convert low-to-medium grade solar energy into electricity and heat.
The higher the temperature level, the higher the electrical conversion efficiency. For this reason, ORC systems are studied in combination with concentrated solar technologies such as in (Taccani *et al.*, 2016) and (Bouvier *et al.*, 2016). In (Villarini *et al.*, 2019), a comparison between the performances of two different solar ORC micro-trigeneration systems based on different solar technologies was carried out. The authors found that when the solar irradiance is low, the use of compound parabolic collectors (CPC) instead of concentrated solar technologies (such as Linear Fresnel Reflectors) brings to higher electrical and thermal energy outputs during wintertime because of the low operating temperatures.
Solar energy is characterized by high hourly and seasonally fluctuations causing challenging dynamic effects to ORC systems and making them operate in off-design conditions. This behavior reflects in

different electrical and thermal power outputs and consequently leads to different profitability of the system.

As far as system modeling is concerned, many researchers in the literature have developed models and ad-hoc subroutines to assess the daily and annual performances of solar ORC systems. For instance, (Calise *et al.*, 2015) developed a model in TRNSYS-EES to investigate the techno-economic performance of a 6 kWe ORC unit coupled with 73.5 m^2 of innovative flat-plate evacuated solar collectors for different locations in the Mediterranean area. Based on their study, the authors found that the efficiency of the ORC does not vary significantly during the year remaining always close to 10% despite the efficiency of the solar field was much lower during the winter. However, as also highlighted by (Ziviani *et al.*, 2014), the variability of the heat source brings ORC systems to work at part-load conditions thus requiring more detailed models. For example, (Manente *et al.*, 2013) developed a detailed off-design model of an ORC system in Simulink by imposing the mass and energy balances for each component and by introducing appropriate performance curves for the main components. The model was then used to find the optimal operational strategy to maximize electricity production in different ambient conditions.

The design and modeling of ORC systems are challenging in solar applications, in which the heat source fluctuates significantly hourly and seasonally in addition to the variation of the ambient temperature. Therefore, the components of the ORC system are forced to operate in off-design conditions and this may result in performance degradation, instabilities, or even failure in rotary machines (Moradi, 2021). The challenges are due to the lack of adequate knowledge about the off-design performances of the components during the system design as the manufacturers usually provide design performances of heat exchangers and limited off-design information of the rotary machines. The latter can be available not only in a different range of off-design conditions compared to the intended application but also for different working fluids. Therefore, the design and the annual performance of solar systems assessed with only the design or the limited off-design specifications of the components may be questionable for their accuracy.

Moreover, the way the system boundary conditions are determined, which are usually based on reasonable assumptions regarding some thermodynamic states of the system, affects the overall accuracy of the modeling. The assumptions in component models and the system boundary identification methods may exacerbate or subside the overall deviation between the model results and the real system off-design performances thus influencing the sizing of the different components at the design stage. The overlap between the component modeling and the system boundary identification method is a gap in the literature seeking for the best approach predicting the annual performances of solar systems.

Therefore, in this paper four modeling approaches are considered combining two component modeling approaches (single-coefficient and empirical) and two system boundary identification methods (fixed temperature pinch and assumption-based). The four models of the micro-ORC system are integrated with the other components of a 4 kWe/50 kWth CCHP ORC system to assess its annual performances. Hence, the paper is structured as follows: after the introduction, Section 2 describes the methods used together with the main characteristics of the models. In Section 3 the main results of the analysis are reported while Section 4 concludes.

2 METHODS AND MODELS

This section firstly reports the method of the present work and then describes the different models used to simulate the solar ORC system. Indeed, the performances of the micro-solar trigeneration system are assessed in TRNSYS® combining the built-in components with the ad-hoc models of the ORC unit developed by the authors in MATLAB®. The system consists of (I) 170 m^2 CPC solar field, (II) a micro-scale 4 kWe/50 kWth non-regenerative ORC unit working with R245fa, (III) two storage tanks (oil tank and water tank) to store the input and output thermal energy of the ORC unit, and (IV) a dry cooler and a natural gas boiler to discharge the excess heat or to supply additional energy to meet the users' thermal demand respectively. Regarding the users' thermal demands, hot water, space heating, and heat to drive the absorption chiller to provide space cooling are included in the model as shown in Figure 1.

Moreover, Table 1 reports the main characteristics of the solar system while further details on the specifications of the other components of the ORC unit are available in (Moradi *et al.*, 2021).

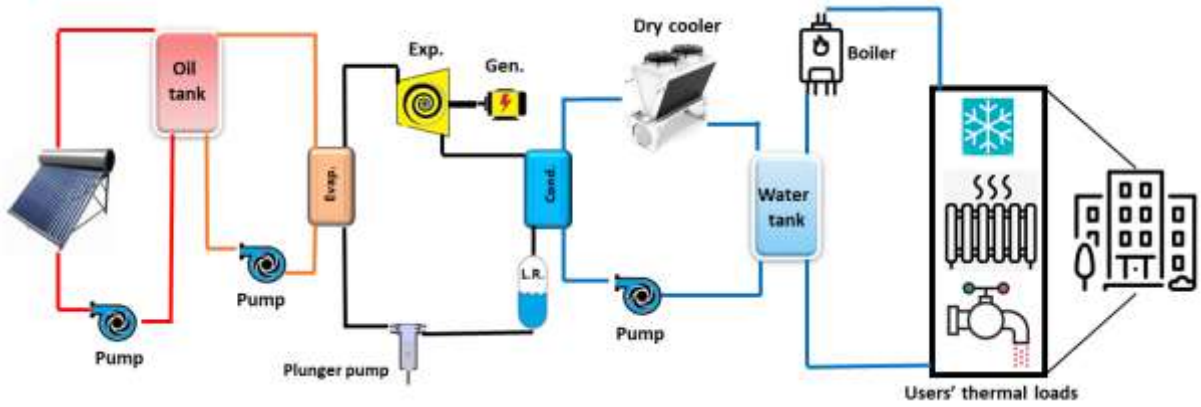

Figure 1: The scheme of the micro-solar ORC system

Table 1: The main characteristics of the integrated solar system

Evacuated tube collectors	Area [m^2]	170
High-temperature storage tank	Volume [m^3]	3
Low-temperature storage tank	Volume [m^3]	5
Heat transfer medium (Texatherm HT22)	Density (at 20°C) [kg/m^3]	885.1
	Operating temperature range [°C]	-45 - 290
	Kinematic viscosity [cSt]	22 at 40°C 3.75 at 100°C
Scroll expander	Built-in volume ratio [-]	4.05
	Swept volume [cc/rev]	36.54
Absorption chiller	$COP = Q_{ev}/Q_{generator}$	0.7

2.1 Modeling of the ORC system

Four models are used in this work to compare the common modeling approaches in annual system-level simulations of ORC systems. These models are different in the way the components are modeled and the way that the system boundaries are determined. Regarding the components, they are modeled empirically using polynomial regression models or by single-coefficient models. The formers are tuned using the experimental data of a micro-scale ORC test bench presented in (Moradi *et al.*, 2021), except for the scroll expander, which is based on the results of the semi-empirical model presented in (Lemort *et al.*, 2009). This choice is due to the relatively low performances of the scroll expander in (Moradi *et al.*, 2021) since it was tested at low shaft speeds which would penalize the net electric efficiency of the integrated system consequently. Therefore, the working conditions of the ORC system are adopted to match with the characteristics of that expander (working at a fixed shaft speed of 2500 rpm) thus resulting in an inevitable extrapolation of the empirical models of the PHEs and the pump. Nevertheless, the results of the models are remained in a feasible range and hence are considered adequate for the scope of the present analysis. Finally, the single-coefficient models of the components are derived from the average of the results of the empirical simulations. Regarding the empirical models, the following points are considered at the same time:

- use of physically relevant variables in the models;
- a physically meaningful trend when an isolated variable in the model alters;
- good accuracy of the model compared to the database used to tune the model.

Regarding the system boundary identification method, the assumption-based model is employed that maintains the preset superheating and subcooling degrees in the evaporator and the condenser using iterative loops as presented in details in (Moradi *et al.*, 2021). In particular, the expander suction pressure is calculated so the mass flow rate produced by the refrigerant pump is almost equal to the

mass flow rate that the scroll expander can devour at the given shaft speed. The expander discharge pressure is calculated so the preset subcooling degree is maintained at the condenser outlet. The preset superheating and subcooling degrees are considered 5 K and 0 K respectively; however, the temperature pinch is controlled in the model and if a cross-temperature occurs, the preset values are increased by the code until the negative temperature pinch is resolved.

Instead, the other method used in this work assumes a fixed pinch between the inlet temperatures of the hot and the cold streams and the refrigerant saturated temperature in the evaporator and the condenser, respectively. This method is to calculate the high and the low pressures of the cycle knowing the heat source and sink temperatures as used in (Cioccolanti *et al.*, 2018).

Despite their differences in calculating the high and low pressure of the cycles, both models calculate the refrigerant mass flow rate (i.e. the refrigerant pump speed) to maintain the preset superheating in an iterative loop. Therefore, the models are numbered as in Table 2 to represent the results clearer.

The summary of the empirical and single-coefficient models is reported in Table 3. The definitions of the performance parameters of the components are presented in Appendix (A), and more details are available in (Moradi *et al.*, 2021). The single-coefficient models are derived as the average of the results of the ORC model I in the range of the heat source and sink temperatures covering both the experimental data reported in (Moradi *et al.*, 2021) and the expected values of the simulation of the solar ORC system: 120-180°C for the heat source and 10-70°C for the heat sink. Only for the pump volumetric efficiency, the ideal value is assumed for simplicity, and because it was above 97.5% in the experiments (Moradi *et al.*, 2021). Finally, the average temperature pinches used in models II & IV are 25.97°C and 18.74°C for the evaporator and the condenser, respectively.

Table 2: The models used to simulate the ORC system

Model number	System model	Components model
I	Assumption-based	Empirical
II	Fixed temperature pinch	Empirical
III	Assumption-based	Single coefficient
IV	Fixed temperature pinch	Single coefficient

Table 3: The empirical and single-coefficient models of the components of the ORC unit

Component	Empirical	Single coefficient
Scroll expander	$FF = f(N_{exp}, P_{su,exp})$	$FF = 96.8\%$
	$\eta_{is,exp} = f(N_{exp}, PR_{exp})$	$\eta_{is,exp} = 80.28\%$
	$\eta_{mech,exp} = f(N_{exp}, PR_{exp})$	$\eta_{mech,exp} = 59.9\%$
Plunger pump	$\eta_{vol,p} = f(N_p)$	$\eta_{vol,p} = 100\%$
	$\eta_{is,p} = f(N_p, T_{su,p}, P_{su,p}, P_{dis,p})$	$\eta_{is,p} = 50\%$
	$\eta_{el,p} = f(N_p, PR_p)$	$\eta_{el,p} = 88.7\%$
Evaporator	$\eta_{th,ev} = f(T_{in,HF}, \dot{m}_{HF})$	$\eta_{th,ev} = 21.79\%$
	$dP_{ev} = 2.7\%$	$dP_{ev} = 2.7\%$
Condenser	$\eta_{th,cd} = f(T_{in,CF}, P_{in,ref}, \dot{m}_{ref})$	$\eta_{th,cd} = 73.58\%$
	$dP_{cd} = 10\%$	$dP_{cd} = 10\%$

2.2 The control logic of the system

The plant is coupled with 3 residential blocks consisting of 4 adjacent apartments each (total area of 1200 m^2) located in Rome. The related space heating and cooling thermal loads are calculated using TRNBuild considering an indoor comfort temperature of 20°C and 24°C in winter and summer, respectively. The hot water demand is calculated using a separated simulation in TRNSYS according to the standard recommendations (Technical Committee CEN/TC 228, 2006).

The condenser of the ORC system, the users' thermal loads, the dry cooler, and the auxiliary boiler interact with the water storage tank. The auxiliary boiler energy consumption is obtained by applying a simple energy balance to maintain the water storage tank temperature within a certain range. The minimum temperature of the water storage tank is controlled depending on the status of the absorption

chiller (on/off) using the auxiliary boiler. Instead, its maximum temperature remains limited using the dry cooler. This is to avoid very high temperatures in the tank and the resulted losses of the produced electric power by the ORC system. Therefore, the operational scenarios of the auxiliary boiler and the dry cooler are as reported in Table 4. The temperature of the water storage tank is set to a range suitable for hot water and space heating when the absorption chiller is off, while this range is considerably higher when it is on according to the minimum temperatures usually needed for the vapor regenerator of the absorption chillers.

Table 4: Operational scenarios of the auxiliary boiler and the dry cooler based on the absorption chiller status

Absorption chiller off				**Absorption chiller on**			
auxiliary boiler on	auxiliary boiler off	dry cooler on	dry cooler off	auxiliary boiler on	auxiliary boiler off	dry cooler on	dry cooler off
$T_{avg,tk}$ = 30°C	$T_{avg,tk}$ = 40°C	$T_{out,tk}$ = 74°C	$T_{out,tk}$ = 70°C	$T_{avg,tk}$ = 60°C	$T_{avg,tk}$ = 70°C	$T_{out,tk}$ = 74°C	$T_{out,tk}$ = 70°C

Regarding the high-temperature pump, it switches on and charges the oil tank when the collector temperature is 10 K higher than the average temperature of the oil tank, while the medium-temperature pump is on and discharges the oil tank when the tank average temperature is above 150°C. When the medium-temperature pump is on, the water pump is on as well and the ORC system is solved until the diathermic oil temperature at the outlet of the tank falls below 120°C. Finally, the dry cooler is on when the conditions in Table 4 are met and the water pump is on simultaneously. Simulations are run for one year with a time step of five minutes.

3 RESULTS AND DISCUSSION

The performance data are recorded at each time step and the values are integrated monthly. It is assumed that the produced electric energy is totally consumed by the users, while the useful produced thermal energy consumed by the users is calculated using the difference between the users' thermal demand and the produced energy by the auxiliary boiler.

$$Q_{th} = Q_{users} - Q_{boiler} \tag{1}$$

Hence, the total thermal efficiency of the solar system is defined as the ratio of the useful produced thermal energy to the users' thermal demand indicating the fraction of the users' thermal demand covered by solar energy:

$$\eta_{th,tot} = \frac{Q_{th}}{Q_{users}} = 1 - \frac{Q_{boiler}}{Q_{users}} \tag{2}$$

The overall efficiency of the trigeneration system to supply the users' electric and thermal energy demands calculated as the following:

$$\eta_{CCHP} = \frac{W_{el.net,ORC} + Q_{th}}{Q_{gain}} \tag{3}$$

where Q_{gain} is the absorbed solar energy by the collectors. The electric energy consumed by the oil pumps, the water pump, and the dry cooler fan are not considered here to focus on the ORC system results modeled using the four modeling approaches. The round trip electric and thermal efficiencies of the solar ORC system are calculated as the following:

$$\eta_{el,ORC} = \frac{W_{el.net,ORC}}{Q_{gain}} \tag{4}$$

$$\eta_{th.ORC} = \frac{Q_{th,cd}}{Q_{gain}} \tag{5}$$

Finally, the thermal efficiency of the solar collectors is calculated using Equation (6):

$$\eta_{th,collector} = \frac{Q_{gain}}{I_{solar}} \tag{6}$$

In the following, the performances of the solar ORC system are presented first using the ORC model I. Then, the impact of the four models of the ORC system is presented by comparing the monthly average values of some performance parameters.

3.1 The system performance using ORC model I

The annual performances of the micro-solar ORC system are presented hereunder using monthly average results in the case of ORC model I. The users' thermal demand and the produced energy by the ORC condenser and the auxiliary boiler are presented in Figure 2 together with the operational time of the ORC system. In wintertime, the auxiliary boiler turns on often while the dry cooler turns on frequently in summer thus penalizing the overall efficiency of the system. Therefore, a better redesign of the system may be needed to achieve higher performance. Nevertheless, useful considerations can be drawn concerning the modeling approaches.

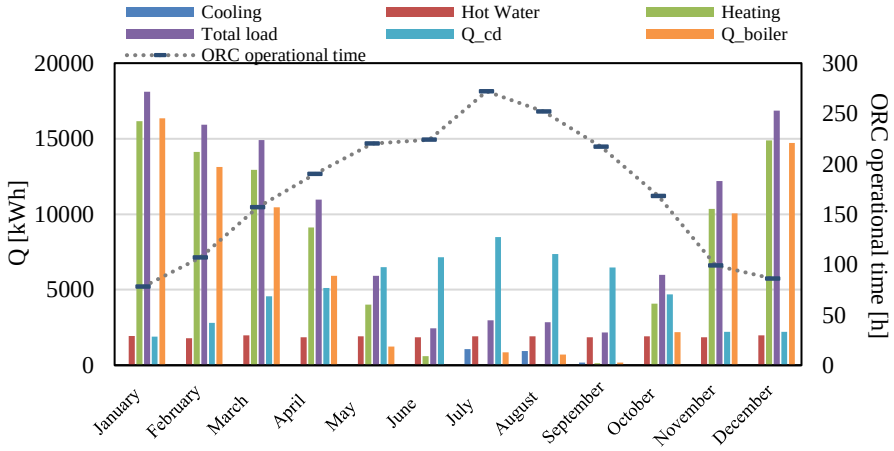

Figure 2: The monthly average thermal energy consumed by the users and produced by the ORC condenser and the auxiliary boiler along with the operational time of the ORC system.

Figure 3 (left) shows the produced net electric energy and useful thermal energy. The produced electric energy is higher in hot months, but the useful thermal energy is lower compared to that in midseason months, which is due to the low thermal demand. In cold months, the thermal demand is high, but the produced thermal load is low because of the low solar radiation.

The overall efficiency of the trigeneration system along with the other efficiencies defined in Equations (2-6) are presented in Figure 3 (right). The system can usefully deliver the gained solar energy in the collectors to the final users in the months when the chiller is off resulting in high CCHP efficiencies. In other words, most of what is produced are then consumed by the users. On the other hand, in the months that the chiller turns on and both the water tank average temperature and the solar radiation are high, large amounts of the produced thermal power are wasted to the ambient by the dry cooler since the cooling thermal load of the absorption chiller is low. Therefore, the system's overall efficiency drops drastically in hot months. Indeed, it can be ameliorated if the cooling load was higher meaning a more uniform distribution of the users' monthly thermal load in a year. However, the total thermal efficiency is higher in hot months indicating that the higher fraction of the users' thermal demand is met by solar energy. Therefore, the system produces more electricity and covers a higher fraction of the users' thermal demand in hotter months.

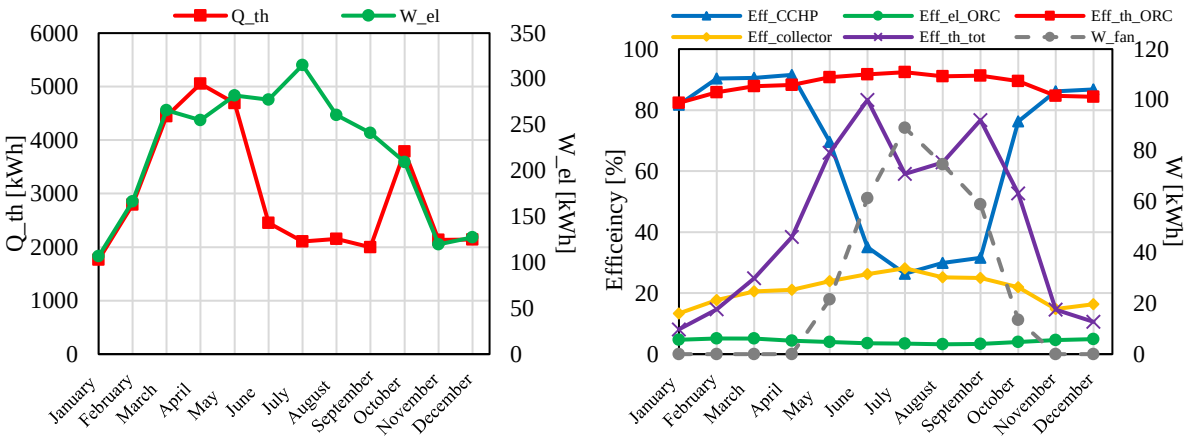

Figure 3: The monthly average produced net electric energy and the useful thermal energy by the ORC unit (left); The system overall efficiency (blue), total thermal efficiency (violet), ORC round trip electric and thermal efficiencies (green & red), collector thermal efficiency (yellow), and fan consumed electric energy (gray) (right).

3.2 The impact of the ORC model

The impact of the modeling approaches of the ORC unit on the performances of the micro-solar ORC system is investigated in terms of the net produced electric energy by the ORC unit and its operational time as in Figure 4. The ORC model has a significant impact on its net produced electric energy, especially in hot months in which the chiller turns on and the average water tank temperature increases. Model II gives considerably lower operational time than the other three models that explains the lower produced net electric energy. This is due to very low pressure ratios imposed on the expander on hot days having fixed temperature pinch in this model thus penalizing the expander performance. The same occurred for model IV, but in the case of single coefficient models, the expander performance is insensitive to pressure ratio and the net electric power remains positive.

Moreover, model III overpredicts the net electric energy of the ORC unit especially in hot months compared to the other three. This is because not only the expander pressure ratio is not calculated so low as in models II & IV but also the expander performances are not penalized in low pressure ratios and remain at the average value. The former avoids a low available thermodynamic work, and the latter neglects the influence on the expander shaft power. Therefore, it produces more electric energy despite its operating hours are the same as for models I & IV.

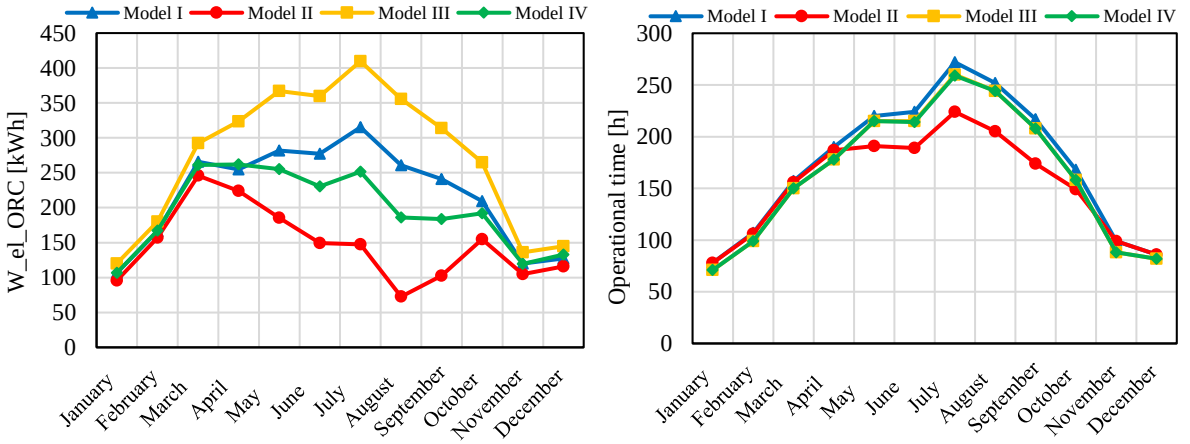

Figure 4: The monthly average net produced electric energy of the ORC unit (left), and the operational time of the ORC unit (right)

It is concluded that assuming model I as the more physically relevant model having the least number of assumptions, model IV that is the simplest one shows the most similar results. This is confirmed in Table 5, which reports a comparative summary of the annual net electric energy produced by the ORC

unit and its annual operation time for the four models. In model IV that is the simplest model, the expander pressure ratio is low reducing the expander produced thermodynamic power, but the expander mechanical efficiency is fixed to an average value that is higher than the empirical values; hence, the opposed impacts of the system and the component modeling methods result in the least discrepancy between models I & IV.

Table 5: the annual net electric energy produced by the ORC unit and its annual operation time for the four models

Parameter	Model I	Model II/ Model I	Model III/ Model I	Model IV/ Model I
$W_{el.net,ORC}$ [MWh]	2.6	0.67	1.24	0.89
Operational time [h]	2070	0.89	0.95	0.95

Finally, despite the significant sensitivity of the net produced electric energy of the ORC unit to the modeling method of the ORC unit, the useful thermal energy does not show a considerable discrepancy resulting in a similar overall efficiency of the systems for all the models. Therefore, the modeling of the expander efficiency and its pressure ratio are more important on the off-design modeling of such systems compared to the modeling of other components and parameters.

4 CONCLUSIONS

A micro-solar ORC system has been simulated annually using TRNSYS® for trigeneration applications considering 12 apartments, 100 m^2 each, located in Rome. The users' thermal demands have been simulated in TRNSYS including the thermal loads of the space heating, hot water, and vapor generator of the absorption chiller. Four different modeling approaches of the ORC unit that are common for annual system-level simulations are developed in MATLAB® to simulate the integrated system.

Firstly, the results have shown the significant impact of the users' thermal load distribution to achieve a well-sized trigeneration system able to operate smoothly with good overall efficiency in all the months of the year. In such conditions, the users' thermal demands do not fluctuate much seasonally resulting in a less operational time of the auxiliary boiler in cold months and of the fan of the dry cooler in the hot months. Nonetheless, the results have shown that the studied CCHP system operates with an average monthly overall efficiency ranging from 26 to 91% with an operational time in the range of 78-272 hours.

Finally, the results of the four ORC models have been compared with each other in terms of the monthly average net electric energy produced by the ORC unit, the operational time, and the overall efficiency. Results have shown that the monthly average net electric energy of the ORC unit is very sensitive to the ORC modeling approach. In particular, the simplest model (model IV) gives the most similar results compared to the model with the least assumption (model I). However, all four models have similar results in terms of the average monthly overall efficiency of the ORC unit. The discrepancy of the models is vividly higher in hot months, in which the chiller turns on. This is because the expander model is very sensitive to low pressure ratios and over-expansion losses penalizing its performance significantly, while it is relatively less sensitive to the under-expansion losses in high pressure ratios. Therefore, the discrepancy in the net electric energy produced by the ORC unit depends on the expander model and its pressure ratio calculation especially in the case of low values such as when the absorption chiller is at service.

Therefore, the results of this study suggest particular attention to the modeling approach of the ORC system integrating with other energy systems due to the complex and two-sided interaction between the system boundary identification method and the component modeling method and their contribution to the overall system results. The findings of this work are particularly interesting for simulation of solar ORC systems at the design stage when no experimental data are available and the knowledge about the performance of the components in off-design conditions is limited.

NOMENCLATURE

T	temperature	(°C)
P	pressure	(Pa)
Q	thermal energy	(kWh)
W	electric energy	(kWh)
I	Total solar Irradiation on the collectors	(kWh)
η/Eff	efficiency	(%)
N	shaft speed	(rpm)
$\dot{m}$	mass flow rate	($kg.s^{-1}$)
C_p	specific heat	($J.kg^{-1}.K^{-1}$)
FF	Filling Factor	(-)
BVR	Built-in Volume Ratio	(-)
PR	Pressure Ratio	(-)
COP	Coefficient Of Performance	(-)

abbreviations

ORC	Organic Rankine Cycle
WHR	Waste Heat Recovery
CCHP	Combined Cooling, Heat and Power

Subscripts

th	thermal/theoretical/thermodynamic
el	electrical
cd	condenser
ev	evaporator
exp	expander
comp	compressor
p	pump
su	suction
dis	discharge
LT	low temperature
ref	refrigerant
HF	hot fluid
CF	cold fluid
is	isentropic
act	actual
meas	measured

Appendix (A): Data reduction

Pump volumetric efficiency:

$$\eta_{vol,p} = \frac{\dot{m}_{meas}}{\dot{m}_{th}} \tag{A1}$$

where the theoretical mass flow rate is calculated as the following:

$$\dot{m}_{th} = \frac{N \cdot SV \cdot \rho_{su}}{60} \tag{A2}$$

Pump isentropic efficiency:

$$\eta_{is,p} = \frac{\dot{W}_{th,is}}{\dot{W}_{th,act}} = \frac{h_{dis,is,p} - h_{su,p}}{h_{dis,p} - h_{su,p}} \tag{A3}$$

Pump electromechanical efficiency:

$$\eta_{el,p} = \frac{\dot{m}(h_{dis} - h_{su})}{\dot{W}_{el,meas}} \tag{A4}$$

Expander isentropic efficiency:

$$\eta_{is,exp} = \frac{\dot{W}_{th,act}}{\dot{W}_{th,is}} = \frac{h_{su,exp} - h_{dis,exp}}{h_{su,exp} - h_{dis,is,exp}} \tag{A5}$$

Expander mechanical efficiency:

$$\eta_{mech,exp} = \frac{\dot{W}_{sh}}{\dot{W}_{th,act}} = \frac{\dot{W}_{sh}}{\dot{m}(h_{su,exp} - h_{dis,exp})} \tag{A6}$$

Expander filling factor:

$$FF_{exp} = \frac{\dot{V}_{meas}}{\dot{V}_{th}} = \frac{\dot{m}/\rho_{su,exp}}{N_{exp} \cdot SV_{comp}/(60BVR)} \tag{A7}$$

Thermal efficiency of the evaporator and the condenser:

$$\eta_{th} = \frac{Q}{Q_{max}} \tag{A8}$$

$$Q_{max} = \dot{m}_{HF} \cdot C_{p,HF}\left(T_{in,HF} - T_0\right) \tag{A9}$$

Where the subscript 'HF' refers to the hot stream in the evaporator (oil) and condenser (refrigerant). T_0 is the assumed minimum temperature that the hot stream can be exploited down to it and it is considered 20°C for the evaporator and 0°C for the condenser.

REFERENCES

Bouvier, J.L., Michaux, G., Salagnac, P., Kientz, T., Rochier, D., 2016. Experimental study of a micro combined heat and power system with a solar parabolic trough collector coupled to a steam Rankine cycle expander: *Sol. Energy*, vol. 134, p. 180–192.

Calise, F., D'Accadia, M.D., Vicidomini, M., Scarpellino, M., 2015. Design and simulation of a prototype of a small-scale solar CHP system based on evacuated flat-plate solar collectors and Organic Rankine Cycle: *Energy Convers. Manag.*, vol. 90, no. Complete: p. 347–363.

Cioccolanti, L., Tascioni, R., Arteconi, A., 2018. Mathematical modelling of operation modes and performance evaluation of an innovative small-scale concentrated solar organic Rankine cycle plant: *Appl. Energy*, vol. 221, p. 464–476.

Lemort, V., Quoilin, S., Cuevas, C., Lebrun, J., 2009. Testing and modeling a scroll expander integrated into an Organic Rankine Cycle: *Appl. Therm. Eng.*, vol. 29, no. 14–15: p. 3094–3102.

Manente, G., Toffolo, A., Lazzaretto, A., Paci, M., 2013. An Organic Rankine Cycle off-design model for the search of the optimal control strategy: *Energy*, vol. 58, p. 97–106.

Moradi, R., 2021. Object-oriented modeling of micro-ORC systems for low-grade waste heat recovery applications: Doctroal thesis, Sapienza University of Rome.

Moradi, R., Habib, E., Bocci, E., Cioccolanti, L., 2021. Component-Oriented Modeling of a Micro-Scale Organic Rankine Cycle System for Waste Heat Recovery Applications: *Appl. Sci.*, vol. 11, no. 5: p. 1984.

Taccani, R., Obi, J.B., De Lucia, M., Micheli, D., Toniato, G., 2016. Development and Experimental Characterization of a Small Scale Solar Powered Organic Rankine Cycle (ORC). In: *Energy Procedia* Elsevier Ltd, p. 504–511.

Technical Committee CEN/TC 228, 2006. Heating systems in buildings — Method for calculation of system energy requirements and system efficiencies — Part 3-1 Domestic hot water systems, characterisation of needs (tapping requirements).:

Villarini, M., Tascioni, R., Arteconi, A., Cioccolanti, L., 2019. Influence of the incident radiation on the energy performance of two small-scale solar Organic Rankine Cycle trigenerative systems: A simulation analysis: *Appl. Energy*, vol. 242, p. 1176–1188.

Ziviani, D., Beyene, A., Venturini, M., 2014. Advances and challenges in ORC systems modeling for low grade thermal energy recovery: *Appl. Energy*, vol. 121, p. 79–95.